Complexity-Reduced Equalization for 200 Gbit/s PON Downstream Systems Based on SSB Modulation and Direct Detection

Yang Tao[1], Huang Xingang[2], Ma Zhuang[2], Zhong Yiming[2], Huang Xiatao[2], Liu Bo[2]

(1. State Key Lab of Information Photonics and Optical Communications, Beijing University of Posts and Telecommunications, Beijing 100876, China;
2. ZTE Corporation, Shanghai 201203, China)

DOI: 10.12142/ZTECOM.202601008

https://kns.cnki.net/kcms/detail/34.1294.TN.20260309.1357.002.html, published online March 10, 2026

Manuscript received: 2024-06-26

Abstract: The 200 Gbit/s passive optical network (PON) is most likely to be the next-generation scheme following 50G PON. The cost-effective direct detection (DD) system is the economical choice. However, larger-capacity DD systems will face much more serious power fading caused by chromatic dispersion (CD) combined with square-law DD and thereby significantly increases the complexity of equalization algorithms. In this paper, a 200 Gbit/s Nyquist 4-level pulse amplitude modulation (PAM4) single side-band (SSB) modulation-DD downlink scheme is designed, and a low complexity quadratic-nonlinear equalizer is proposed for this system. The computational complexity of the quadratic nonlinear equalizer is about 28% of that of the conventional Volterra nonlinear equalizer, while still exhibiting excellent nonlinear equalization ability. Simulation results for the 200 Gbit/s system with 20 km fiber transmission show that it can achieve a power budget of 29 dB, while a 30.4 dB power budget is obtained in the 50 Gbit/s experimental transmission.

Keywords: 200 Gbit/s passive optical network; single side band modulation; direct detection; equalization

Citation (Format 1): Yang T, Huang X G, Zhong Y M, et al. Complexity-reduced equalization for 200 Gbit/s PON downstream systems based on SSB modulation and direct detection [J]. ZTE Communications, 2026, 24(1): 56 - 64. DOI: 10.12142/ZTECOM.202601008

Citation (Format 2): T. Yang, X. G. Huang, Y. M. Zhong, et al. "Complexity-reduced equalization for 200 Gbit/s PON downstream systems based on SSB modulation and direct detection," *ZTE Communications*, vol. 24, no. 1, pp. 56 - 64, Mar. 2026. doi: 10.12142/ZTECOM.202601008.

1 Introduction

Passive optical networks (PON) based on power splitting provide a cost-effective optical access solution for delivering broadband access to diverse end-users. So far, most commercially deployed PONs are time-division multiplexed (TDM). The optical line terminal (OLT) at the central office is connected through an optical distribution network (ODN) with many optical network units (ONUs) at the user side using passive optical power splitting[1]. Gigabit passive optical networks (GPON) have dominated the early PON deployment, offering 100 Mbit/s broadband access services. To provide gigabit services, network operators have been upgrading the networks to 10G PON systems over the past decade. After 10G PON, ITU-T started to study PON technologies above 10 Gbit/s in 2016, and officially started to formulate the high-speed PON standard based on a 50 Gbit/s line rate in 2018. In September 2021, the first edition of the 50G PON standard was officially released by ITU-T. At present, with the rise of various emerging network applications, such as cloud storage and computing, AR/VR, 3D video, and IPTV, higher requirements are placed on the transmission capacity of PON systems. It can be expected that 50G PON will soon be insufficient to meet the needs of users, and the rapid growth of broadband access demand urges the access network to develop toward a higher line rate exceeding 100 Gbit/s. Generally speaking, the compound annual growth rate of user bandwidth demand is about 20%, increasing four- to fivefold every 8 to 10 years. Given that operators typically upgrade PON generations on an 8- to 10-year cycle, the line rate of the next-generation high-speed PON following 50G PON is very likely to be 200 Gbit/s, which also meets the rhythm and bandwidth requirements of PON network evolution.

Up to now, considering the system cost and energy efficiency, the system based on intensity modulation and direct detection (IM-DD) has been the best choice for PON systems. Unlike coherent detection, which requires a local oscillator

This work was supported by ZTE Industry-University-Institute Cooperation Funds under Grant No. HC-CN-20230105001 and National Natural Science Foundation of China under Grant No. 62001045.

and a complex receiver structure, IM-DD only needs a photodiode for detection at the receiving end, significantly reducing the system cost. For operators, it is necessary to upgrade the system without changing the existing ODN. To date, research on high-speed IM-DD transmission has been extensively conducted. To cope with the pressure of rate upgrade and device bandwidth improvement, IM-DD technology will combine with a series of advanced multilevel signal modulation technologies to carry more bits per unit bandwidth. Transmissions of 100 Gbit/s and above per wavelength have been reported by using various modulation formats including 4-level pulse amplitude modulation (PAM4), discrete multitone (DMT), and carrier-free amplitude-phase modulation (CAP)[2-6]. Among these, PAM4 is considered the mainstream candidate because of its simple configuration, low cost, and low power consumption[7]. The next-generation IM-DD-based high-speed PON systems are expected to work in the C-band with lower link loss than that of the O-band, which not only alleviates the current spectrum resource shortage[8], but also allows the compensation of link impairments such as fiber dispersion and nonlinear distortion through digital signal processing (DSP). In addition, using a small and easy-to-integrate semiconductor optical amplifier (SOA) can ensure sufficient power budget while further reducing system costs[9].

However, as optical access networks evolve toward a higher line rate exceeding 100 Gbit/s per wavelength, the transmission of IM-DD systems over the C-band optical fiber will be seriously affected by the chromatic dispersion (CD) effect. At high symbol rates, the system faces frequency-selective power fading, which will lead to serious degradation in receiver sensitivity and insufficient power budget[10]. Equalization technology is considered an effective solution to eliminating intersymbol interference (ISI) caused by device bandwidth limitation and CD. Among various techniques, feed-forward equalizers (FFE) and decision feedback equalizers (DFE) are widely used[11]. These equalizers have simple structures and low power consumption, but they cannot compensate for serious nonlinear damage. In contrast, the Volterra nonlinear equalizer (VNLE) can effectively compensate for both linear and nonlinear impairments originating from fiber channels and the square-law direct detection. However, its complex structure and high computational complexity (i.e., the cost and power consumption of hardware circuit implementations) make it difficult to apply the algorithm directly to future ultra-high-speed IM-DD PON systems.

To reduce the bandwidth requirements of key devices and mitigate power fading in high-speed IM-DD systems, a novel 200 Gbit/s Nyquist PAM4 single side-band (SSB)-DD downstream system is proposed in this paper. By analyzing the forms and characteristics of nonlinear damage in SSB-DD systems, we reasonably simplify the VNLE and propose a quadratic nonlinear equalizer with significantly reduced complexity. Simulation results show that the proposed equalizer can effectively compensate for nonlinear impairments in SSB-DD systems, and the computational complexity is equivalent to that of a linear equalizer. Using the proposed equalizer, the 200 Gbit/s simulation results over 20 km fiber transmission show that the system can achieve a power budget of 29 dB, and a 50 Gbit/s transmission experiment over 20 km yields a power budget of 30.4 dB at a bit error ratio (BER) threshold of 10^{-2}.

2 Principle of 200 Gbit/s PON Downstream Scheme

2.1 200 Gbit/s PON Downlink System Scheme

On the OLT side, if the bitrate is increased from 50 Gbit/s to 200 Gbit/s using a conventional non-return-to-zero/ on-off keying (NRZ/OOK) binary modulation format, optoelectronic devices with bandwidths of 100 GHz to 120 GHz are required, which is obviously extremely difficult and costly in practical applications. Therefore, it is necessary to adopt a high-order modulation format for the downlink transmission of the next-generation 200 Gbit/s PON systems to relax the bandwidth requirements of the devices. To keep low cost and achieve a high power budget, a 200 Gbit/s Nyquist PAM4 SSB-DD PON downlink transmission scheme is designed, as shown in Fig. 1.

To ensure an adequate power budget and acceptable device cost, the scheme adopts PAM4 modulation and performs Nyquist pulse shaping with a roll-off factor of 0.1 to further compress the signal spectrum, thereby reducing the bandwidth requirement of the device while minimizing the CD impact. Due to the limitation of high-speed digital-to-analog converters (DAC) in practical applications, only two-times waveform upsampling is considered. Because the direct detection system only detects light intensity information and is not sensitive to phase information, the system has high tolerance to the laser linewidth. As a result, we can choose a distributed feedback laser (DFB) as the light source at the transmitting end. Compared with generating single-sideband modulation signals based on a single dual-drive Mach-Zehnder modulator (MZM) with increased device cost on the OLT side, using IQ-MZM to generate single-sideband modulation signals in the form of optical auxiliary carriers can adjust the carrier-to-signal power ratio (CSPR) more flexibly to ensure optimal overall system performance. Fortunately, due to the point-to-multipoint nature of PON, the overall cost of the system will not increase significantly.

Here, let $s(t)$ be the original zero-mean PAM4 RF drive signal, and the drive voltage applied to the upper and lower arms of each MZM be $v(t) = s(t) + v_{dc}$. In the case of carrier suppression modulation, the v_{dc} bias voltage is set to the minimum transmission point, that is, the zero point of the power transfer function and the field transfer function. Then, the relationship between the input and the output light fields of MZM is:

$$E_{\text{out}}(t) = E_{\text{in}}(t) \times \cos\left(\frac{s(t)}{V_\pi}\pi - \frac{\pi}{2}\right) = E_{\text{in}}(t) \times \sin\left(\frac{s(t)}{V_\pi}\pi\right).$$

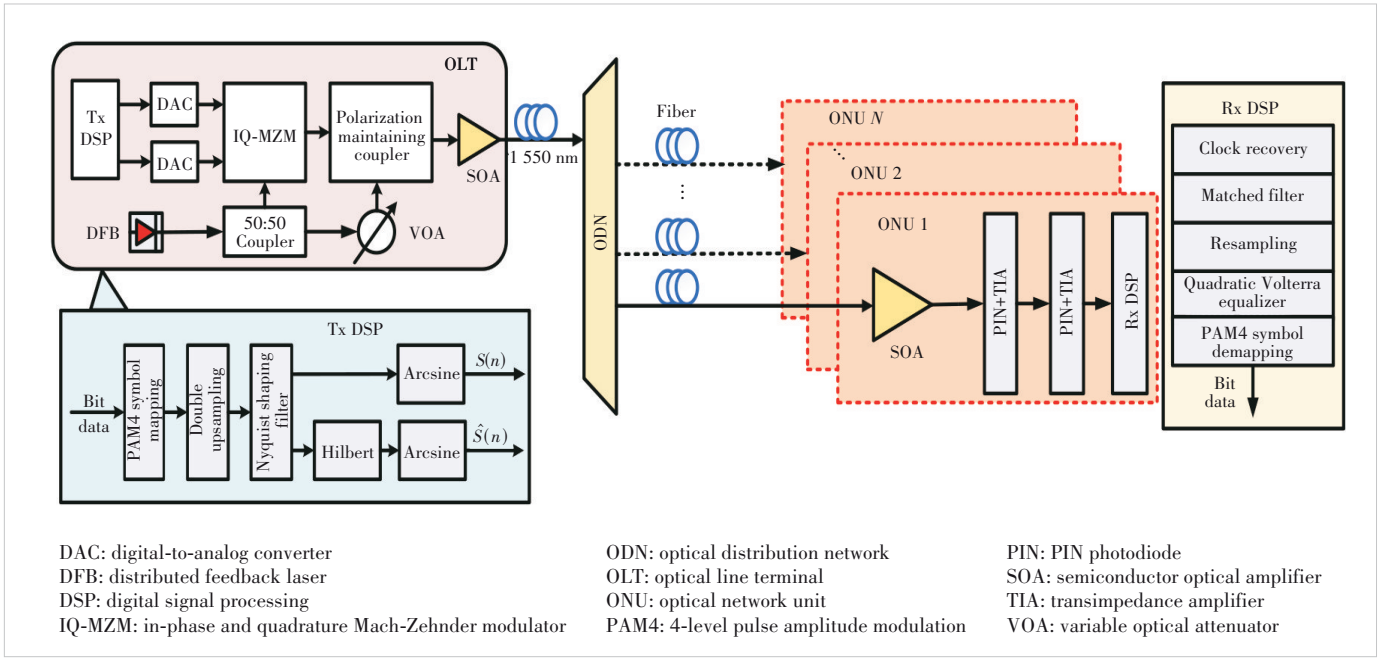

DAC: digital-to-analog converter
DFB: distributed feedback laser
DSP: digital signal processing
IQ-MZM: in-phase and quadrature Mach-Zehnder modulator
ODN: optical distribution network
OLT: optical line terminal
ONU: optical network unit
PAM4: 4-level pulse amplitude modulation
PIN: PIN photodiode
SOA: semiconductor optical amplifier
TIA: transimpedance amplifier
VOA: variable optical attenuator

Figure 1. 200 Gbit/s Nyquist PAM4 SSB-DD PON downlink system scheme

It can be seen that the modulation curve of the MZM is in the form of sine/cosine, and the signal will produce nonlinear distortion at both ends of the modulation dynamic range. To fully utilize the dynamic range of the MZM and maximize the system power budget, it is necessary to perform pre-distortion processing in the arcsine form before the OLT side signal enters the IQ-MZM to overcome the nonlinear effect of the MZM. Finally, an SOA is used to amplify the optical signal in the C-band before fiber transmission.

Generally, compared with a PIN photodiode at the same bandwidth, an avalanche photodiode (APD) offers significantly higher receiver sensitivity. However, on the ONU side, as the bitrate increases to 200 Gbit/s, APD also faces problems of insufficient device bandwidth and constrained gain. As the APD bandwidth increases, the gain decreases, and the sensitivity advantage over the PIN photodiode + transimpedance amplifier (PIN+TIA) scheme diminishes. To sum up, in a 200 Gbit/s PON downlink system, the use of PIN+TIA for photoelectric detection is both cost-effective and feasible for practical implementation. Before entering the PD, the optical signal first goes through an SOA for amplification. The sampling rates of the ADC and DAC are the same, which is twice the symbol rate, that is, 200 GSa/s. The receiver-side DSP processing flow on the ONU side includes clock recovery, matched filtering, double down sampling, and the proposed quadratic Volterra equalization.

2.2 Analysis of Nonlinear Damage in SSB-DD systems

The optical field expression of SSB signals generated by optical transmitters can be written as:

$$E_{\mathrm{SSB}}(t) = b + a[s(t) + \mathrm{jHT}[s(t)] = b + a \cdot c(t) \quad (1),$$

where a and b are complex numbers, so that $|a|^2 + |b|^2 = 1$ is used to constrain the average power of optical SSB signals to keep it constant; $s(t)$ is a real baseband signal, $\mathrm{HT}[\cdot]$ represents the Hilbert transform, and $c(t) = s(t) + \mathrm{jHT}[s(t)]$. $\mathrm{HT}[s(t)]$ can be expressed as $-\mathrm{jsign}(\omega)S(\omega)$ in the frequency domain. $s(t)$ is a real signal that satisfies $S(-\omega)^* = S(\omega)$ in the frequency domain. Therefore, all the information of $c(t)$ is contained on one side of the spectrum, such as the positive frequency side, which can be expressed as $C(\omega) = S(\omega)U(\omega)$, and $U(\omega)$ is a unit step function. After the optical SSB signal is transmitted through fibers, the received optical power can be expressed as[12]:

$$\begin{aligned} P_{\mathrm{Rx}}(t) &= \left|(b + a \cdot c(t)) \otimes h_{CD}(t)\right|^2 = \\ &\left|b + a \cdot c(t) \otimes h_{CD}(t)\right|^2 = \\ &|b|^2 + |a||b|\left[c(t) \otimes h_{CD}(t)\mathrm{e}^{\mathrm{j}\gamma} + c^*(t) \otimes h_{CD}^*(t)\mathrm{e}^{-\mathrm{j}\gamma}\right] + \\ &|a|^2\left|c(t) \otimes h_{CD}(t)\right|^2 = A'(t) + B'(t) + C'(t) \end{aligned} \quad (2).$$

In Eq. (2), $\gamma = \phi_b - \phi_a$ denotes the phase difference between b and a; the first term $A'(t) = |a|^2$ denotes the DC component, the second term $B'(t)$ has a useful signal $c(t)$, and the third term $C'(t) = |a|^2\left|c(t) \otimes h_{CD}(t)\right|^2$ denotes the signal-to-signal beat interference (SSBI) introduced by direct detection after transmission through the optical fiber. If $|a||b|$ is omitted for simplicity, the Fourier transform of $B'(t)$ is $B'(\omega) = C(\omega)H_{CD}(\omega)e^{\mathrm{j}\gamma} + C^*(-\omega)H_{CD}^*(-\omega)e^{-\mathrm{j}\gamma}$. Therefore,

$H_{CD}(\omega)e^{j\gamma} = G(\omega)$ and $B'(\omega)$ can be written as:

$$B'(\omega) = S(\omega)U(\omega)G(\omega) + S^*(-\omega)U^*(-\omega)G^*(-\omega) = S(\omega)\left(U(\omega)G(\omega) + U(-\omega)G^*(-\omega)\right) = S(\omega)M(\omega) \quad (3).$$

$H_{CD}(\omega) = H_{CD}(-\omega)$, and $M(\omega)$ can be summed up as:

$$M(\omega) = e^{j\mathrm{sign}(\omega)\left(\frac{1}{2}\beta_2\omega^2 L + \gamma\right)} \quad (4).$$

The inverse Fourier transform of $M(\omega)$ is a real value, which is expressed as $m(t)$. Since $C'(t)$ can be expressed as $|a|^2\left|c(t) \otimes h_{CD}(t)e^{j\gamma}\right|^2$ and $c(t)$ contains only positive spectral components, Eq. (2) can be rewritten as:

$$P_{\mathrm{Rx}}(t) = |b|^2\left(1 + \frac{|a|}{|b|}s(t) \otimes m(t) + \frac{|a|^2}{|b|^2}\left|c(t) \otimes m(t)\right|^2\right) \quad (5).$$

Obviously, the greatest advantage of SSB-DD is the elimination of the power fading effect. No power fading means that $m(t)$ is reversible, expressed as $m^{-1}(t)$. Therefore, transmission impairments can be effectively compensated by equalization algorithms.

In Eq. (5), $|b|^2$ denotes the power of the carrier, $|a|^2$ denotes the power of the signal, and $|b|^2/|a|^2$ denotes the carrier-to-signal power ratio (CSPR). $|a|^2/|b|^2$ can be expressed as 1/CSPR, and then Eq. (5) can be rewritten as:

$$P_{\mathrm{Rx}}(t) = |b|^2\left(1 + \frac{1}{\sqrt{\mathrm{CSPR}}}s(t) \otimes m(t) + \frac{1}{\mathrm{CSPR}}\left|c(t) \otimes m(t)\right|^2\right) \quad (6).$$

As can be seen from Eq. (6), SSBI becomes severe when the CSPR is too low. Although both the effective signal and SSBI decrease with increasing CSPR, the reduction rate of SSBI is significantly higher. When the CSPR is excessively high, the proportion of carrier power will be too large, which leads to a degraded signal-to-noise ratio (SNR). Consequently, the system sensitivity deteriorates. Hence, there is an optimal CSPR.

2.3 Principle of Low Complexity Nonlinear Equalizer

Traditional FFE and DFE feature simple structure and low power consumption, which can effectively compensate for linear distortion but cannot mitigate serious nonlinear impairments. According to Eqs. (1) and (5), both double sideband modulation and single sideband modulation signals transmitted through optical fiber suffer from SSBI, due to the square law detection of DD receivers, which causes signal distortion. VNLE can compensate for the nonlinear distortion, but it significantly increases the complexity of the equalizer, making it unsuitable for cost-sensitive ONU applications. Meanwhile, when the symbol rate is very high, the large number of tap coefficients renders VNLE impractical for real-time implementation[13].

Different from DSB intensity modulation, the SSBI in SSB-DD systems only contains the second-order term and avoids the power fading effect. Thus, the second-order nonlinear distortion becomes the main factor affecting the transmission performance, so the second-order VNLE is sufficient for effective compensation.

The output of the n-th sample of the second-order VNLE can be expressed as[14]:

$$y(n) = \sum_{m=0}^{L_1-1} w_1(m)x(n-m) + \sum_{l=0}^{L_2-1}\sum_{k=0}^{l} w_2(l,k)x(n-l)x(n-k) \quad (7),$$

where $x(n)$ is the n-th input sample, L_p and w_p are the memory length and kernel weight of order p ($p = 1, 2$), respectively. The second term on the right side of Eq. (7) denotes the nonlinear equalizer including the self-beat frequency term and the cross-beat frequency term, and its tap number is $L_2(L_2 + 1)/2$. Obviously, with the increase of L_2, the computational complexity of VNLE grows significantly.

Because of the square law detection of the DD receiver, the beat frequency term between signals is the most important nonlinear damage term. Therefore, by considering only the second-order distortion in Eq. (7), the second-order VNLE can be further simplified to a quadratic nonlinear equalizer (QNLE), which is expressed as:

$$y(n) = \sum_{m=0}^{L_1-1} w_1(m)x(n-m) + \sum_{l=0}^{L_2-1} w_2(l)x^2(n-l) \quad (8).$$

Obviously, the QNLE is much simpler than the second-order VNLE, as the number of taps in the second term is reduced from $L_2(L_2 + 1)/2$ to L_2. Eq. (8) indicates that under low dispersion conditions, the nonlinear term approximately contains only the square term of the signal. It should also be noted that the influence of fiber dispersion on linear and nonlinear terms is different, which needs to be compensated at the receiving end respectively. In short-range transmission, the self-timer frequency is dominant in the nonlinear terms of SSB-DD reception, so it is considered that the second term $\sum_{l=0}^{L_2-1} w_2(l)x^2(n-l)$ in Eq. (8) can compensate for the nonlinear damage. In the single sideband field modulation system, because there is no power fading, $M(\omega) = e^{j\mathit{sign}(\omega)\left(\frac{1}{2}\beta_2\omega^2 L + \gamma\right)}$, whose inverse Fourier transform, expressed as $m(t)$, is a real value; and there is a reversible $m^{-1}(t)$, so the linear term $s(t) \otimes m(t)$ can be compensated by $\sum_{m=0}^{L_1-1} w_1(m)x(n-m)$ in Eq. (8).

When equalization performance is equivalent, computa-

tional complexity becomes a key indicator for evaluating the quality of an equalizer. Because multiplication operations are significantly more computationally expensive than addition operations, the computational complexity can be judged by the number of multiplications in the equalizer. The computational complexity of the complete second-order Volterra equalizer can be expressed as:

$$M = L_1 + L_2(L_2 + 1)/2 \quad (9),$$

where L_1 represents the number of taps of the first-order term, and L_2 represents that of the second-order term. The computational complexity of the proposed QNLE can be expressed as:

$$M' = L_1 + L_2 \quad (10).$$

By comparing Eqs. (9) and (10), it can be found that the quadratic Volterra equalizer reduces the computational complexity from quadratic to linear growth, thus greatly reducing the computational complexity.

3 Simulation Setup and Results

The simulation setup is shown in Fig. 2. At the transmitter, a binary pseudo-random bit sequence goes through PAM4 symbol mapping, two-times up-sampling, symbol shaping, and spectrum compression using a root raised cosine filter with a roll-off factor of 0.1. The shaped signal is transformed into its real and imaginary parts via the Hilbert transform. After this processing, the two signals are sent to the IQ modulator following DAC to modulate the optical single sideband signal. The modulated signal is amplified by an SOA and then enters the optical fiber for transmission. The variable optical attenuator (VOA) on the transmitter side is used to control the power of the optical carrier signal and thus adjust the CSPR. The optical signal is further amplified using an SOA as a preamplifier, and the noise outside the signal spectrum is filtered by an optical band-pass filter (OBPF) before PD detection at the receiver. The received optical power is adjusted by another VOA. The electrical signals directly detected by the PD (55 GHz 3 dB bandwidth) are processed offline after passing through the ADC. The receiver DSP includes the Gardner clock recovery algorithm, matched filtering, downsampling, the low-complexity quadratic nonlinear equalizer, symbol de-mapping, and BER calculation. Table 1 shows the main simulation parameters of the system.

CSPR is one of the key parameters of the system. If the CSPR is too high, the proportion of carrier power will be too large, which degrades receiver sensitivity. Conversely, if the CSPR is too low, the SSBI impairment will be too strong to be effectively mitigated at the ONU side, which also degrades receiver sensitivity. Therefore, there is an optimal CSPR value that maximizes receiver sensitivity.

First, the BER varies with CSPR under the condition of 20 km optical fiber transmission. The input optical power is 0 dBm to avoid exciting nonlinear effects in the fiber, while the average received optical power is −10 dBm. A 71-tap FFE equalizer is employed at the receiver. Since the SSBI impair-

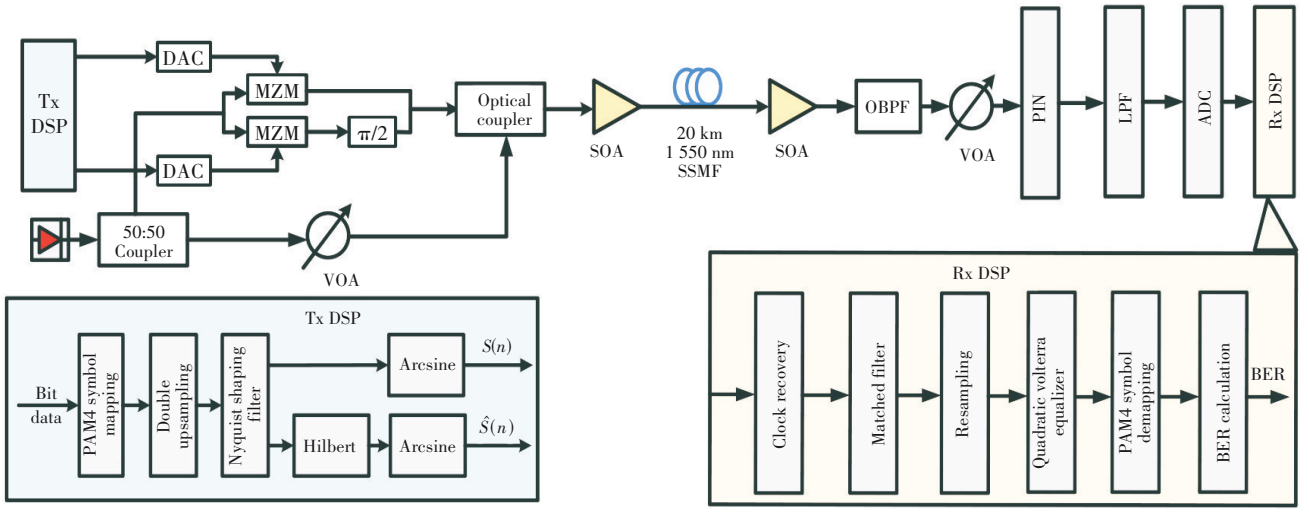

ADC: analog-to-digital converter
BER: bit error ratio
DAC: digital-to-analog converter
DSP: digital signal processing
LPF: low-pass filter
MZM: Mach-Zehnder modulator
OBPF: optical band-pass filter
SOA: semiconductor optical amplifier
VOA: variable optical attenuator
PAM4: 4-level pulse amplitude modulation
SSB: single side-band
PD: Photodiode
PIN: PIN photodiode

Figure 2. Simulation setup of 200 Gbit/s Nyquist PAM4 SSB transmission over 20 km SSMF

Table 1. Main parameters of simulation system

Parameter	Value	Parameter	Value
Bit rate	200 Gbit/s	DAC/ADC sampling rate	200 GSa/s
DAC/ADC ENOB	8	Laser linewidth	10 MHz
MZM extinction ratio	20 dB	SOA noise figure	7.5 dB
Dispersion coefficient	16.5 ps/nm/km	PIN responsiveness	0.8 A/W
PIN thermal noise	1.2e-11 A/Hz^(1/2)	Receiver bandwidth	55 GHz

ADC: analog-to-digital converter
DAC: digital-to-analog converter
ENOB: effective number of bits
MZM: Mach-Zehnder modulator
PIN: PIN photodiode
SOA: semiconductor optical amplifier

ment is also related to dispersion, its impact differs between back-to-back (BtB) and 20 km transmission scenarios. The 20 km transmission results are more representative, as they primarily involve dispersion and SSBI impairments in the system. Since the theoretical sensitivity under BtB conditions is −10 dBm, this paper first optimizes the CSPR around −10 dBm received power. The FFE equalizer can mitigate linear ISI caused by dispersion, but it cannot effectively equalize the nonlinear impairment of SSBI. Therefore, after equalization, there will be residual SSBI impairment, and the size of SSBI impairments is dependent on the system CSPR. In addition, the measured BER curve trend can better reflect the influence of CSPR change on receiver sensitivity, when the received optical power is low. As shown in Fig. 3, for a transmission distance of 20 km, the system achieves the lowest BER and optimal performance when the CSPR is 13 dB.

Next, the relationship between launched power and BER is simulated under the transmission condition of 20 km. To ensure that the change of BER is caused only by power variation (excluding receiver noise influence), the received power is set to 0 dBm. As shown in Fig. 4, with the increase of launched power, fiber nonlinearity is gradually excited, which leads to the system performance degradation. When the launched power exceeds 10 dBm, nonlinear effects become significant. Therefore, 10 dBm is selected as the maximum launched power and used as the condition for subsequent simulations.

Fig. 5 depicts the BER versus different first-order and second-order tap lengths at a received optical power (ROP) of −9 dBm, using the proposed low-complexity quadratic nonlinear equalizer. To determine the optimal tap configuration in the vicinity of the sensitivity, the received power is fixed at −9 dBm. It can be seen that the quadratic nonlinear equalizers with 61 first-order tap lengths and 21 second-order tap

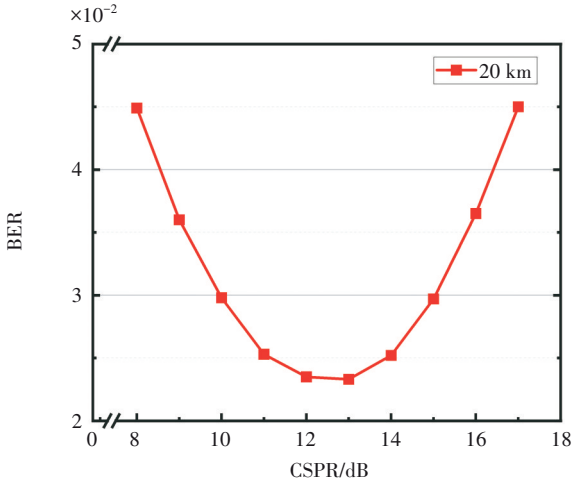

BER: bit error ratio CSPR: carrier-to-signal power ratio

Figure 3. BER versus CSPR under a 20 km transmission simulation

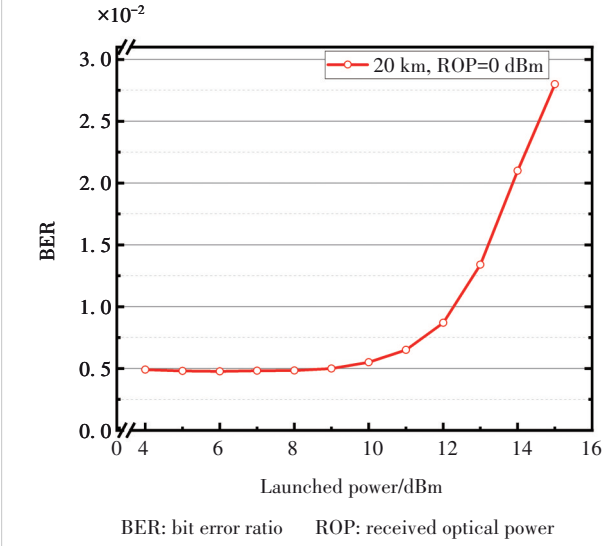

BER: bit error ratio ROP: received optical power

Figure 4. Launched power versus BER

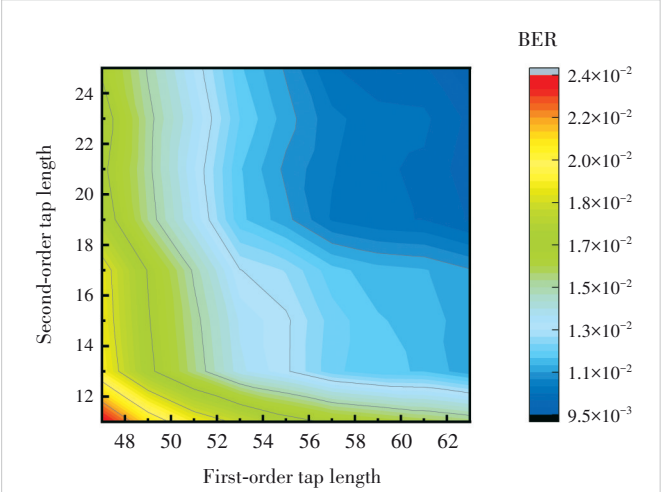

BER: bit error ratio

Figure 5. BER versus filter length at −9 dBm received optical power

lengths achieve a bit error rate threshold of 10^{-2}. As discussed in Section 2, the distortion of the SSB-DD system in the C-band mainly comes from inter-symbol interference caused by dispersion and second-order SSBI, so the quadratic nonlinear equalizer can effectively equalize it. Because the first-order tap length is 61 and the second-order tap length is 21, the ratio of the tap numbers of the quadratic nonlinear equalizer to that of the Volterra nonlinear equalizer is 82/292 (approximately 28.1%). This means that the quadratic nonlinear equalizer can significantly reduce the computational complexity. In addition, the results imply that increasing the number of second-order taps can lead to substantial complexity reduction.

Fig. 6 shows the 200 Gbit/s Nyquist PAM4 SSB transmission over a 20 km standard single-mode fiber (SSMF), achieving a 29 dB total link power budget at a BER of 10^{-2}, taking into account 10 dBm launched power.

4 Experiment and results

The experimental platform is shown in Fig. 7. Due to the bandwidth limitations (14 GHz) of the IQ modulator used in the lab, a 200 Gbit/s transmission experiment remains challenging, and thus our experiment was carried out at a symbol rate of 25 GBaud. The OLT part mainly includes an AWG, an optical IQ modulator, a 1 550 nm DFB laser, a 50∶50 2×1 coupler, a polarization controller, and an adjustable attenuator. First, offline Tx DSP is programmed in MATLAB at the originator. Random bit sequences are generated and mapped to PAM4 symbols (normalized from −1 to 1). The optical IQ modulator operates in both linear and nonlinear regions. If the amplitude of the input signal is too large, it will enter the nonlinear region. Consequently, Tx DSP needs to perform nonlinear pre-distortion of the modulator to resist the nonlinear impairment of the IQ modulator. The generated sequence is divided into two parts, and one of the sequences is subjected to Hilbert transformation. Finally, the two sequences are imported into the arbitrary waveform generator (AWG) as I and Q columns at the same time. In the offline experiment, a Keysight M8194A AWG (3 dB bandwidth: 45 GHz, sampling rate: 120 GSa/s with two channels active) is used to generate 2-channel signals, which work with a Coherent Solutions IQ Transmitter-SP-ABC to realize single-polarization carrier suppression optical modulation. To modulate the optical domain single sideband and control the power ratio of the carrier signal, the output light of the laser was split into two paths via a 50∶50 optical coupler. One path is used as the modulation light source of the IQ modulator, and the other serves as the optical carrier. An adjustable optical attenuator is used to adjust the optical power. The CSPR of the system can be obtained by measuring the power of the output optical signal of the IQ modulator first, and then measuring the output optical power of the adjustable optical decay. After that, the optical carrier signal passes through a polarization controller to keep the polarization state of the output optical signal of the IQ modulator consistent. Finally, it is coupled with the output optical signal of the IQ modulator through a 50∶50 2×1 optical coupler, and then enters the optical fiber for transmission with an SOA power amplifier with a transmit power of 10 dBm.

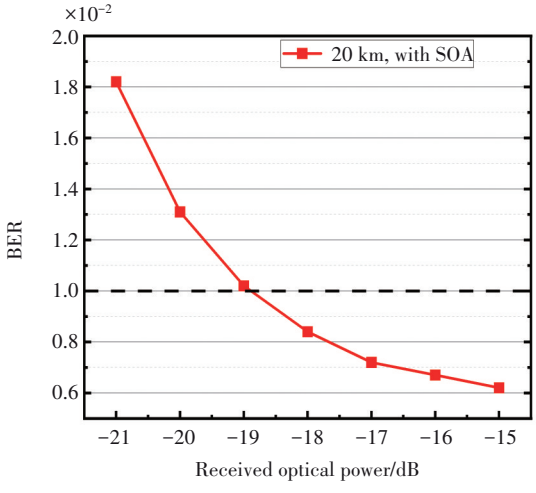

BER: bit error ratio SOA: semiconductor optical amplifier

Figure 6. BER vs ROP under a 20 km transmission simulation

The ONU part mainly includes a PD detection module and a sampling oscilloscope. The optical signal arriving at the ONU first passes through an SOA preamplifier, then through the PD detection module, and is subsequently sampled by the oscilloscope. The responsivity of the PD is 0.65 A/W, and the 3 dB bandwidth is 36 GHz. The signal is sampled by a sampling oscilloscope (LabMaster 10-59Zi-A). When using only one channel, it operates with a sampling rate of 160 GSa/s, a 3 dB bandwidth of 59 GHz, and a resolution of 8 bits. At present, the main DSP algorithm for off-line processing includes matched filtering, double down-sampling, and second-order Volterra equalization. Finally, decision decoding is performed in the data recovery module to restore the original transmitted data, and the error statistics are carried out.

The experimental relationship between BER and CSPR for 20 km transmission is illustrated in Fig. 8, using the same 71-tap FFE configuration as in the simulation. First, the BER varies with CSPR in the case of 20 km fiber transmission with an average received optical power of −20 dBm. As analyzed in Sections 2.3 and 3, while FFE can mitigate linear ISI, the nonlinear SSBI remains a dominant impairment that depends on the CSPR. The BER performance under experimental conditions (20 km transmission) is more representative of these combined effects. As shown in Fig. 8, the experimental system achieves the optimal BER at a CSPR of 11 dB. This is slightly lower than the 13 dB CSPR observed in simulation (see Fig. 3), likely due to the additional bandwidth constraints and noise characteristics of the physical IQ modulator and SOA used in the experimental setup. Therefore, a CSPR of 11 dB

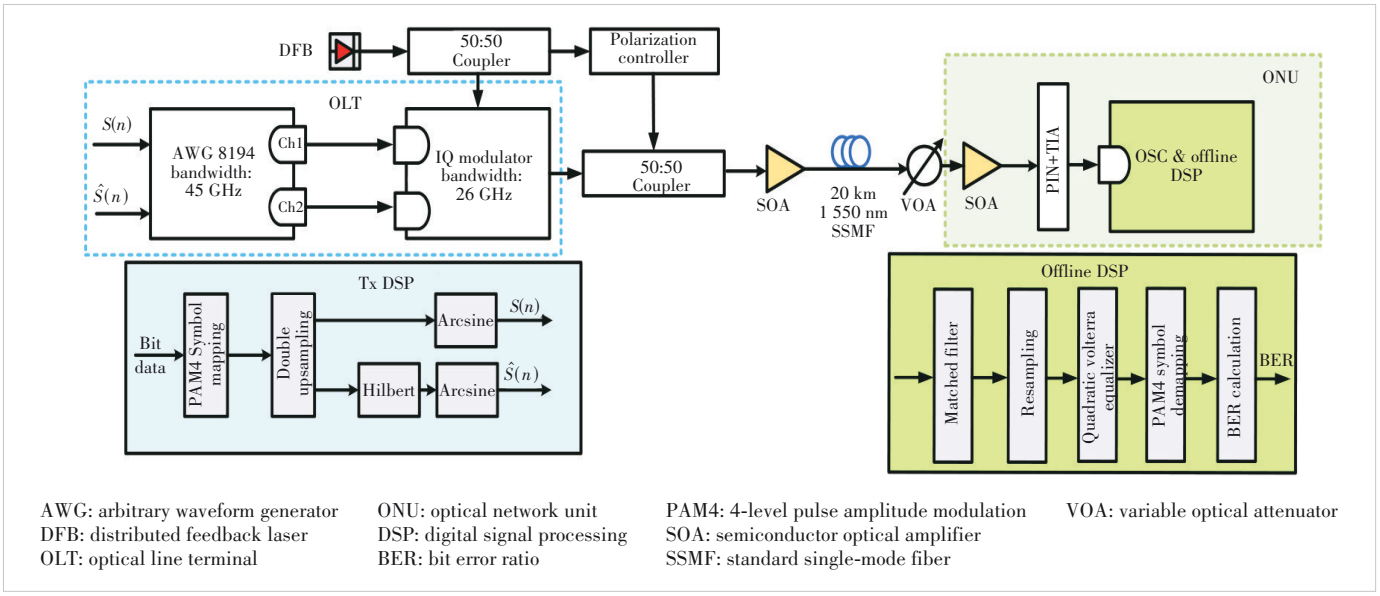

AWG: arbitrary waveform generator
DFB: distributed feedback laser
OLT: optical line terminal
ONU: optical network unit
DSP: digital signal processing
BER: bit error ratio
PAM4: 4-level pulse amplitude modulation
SOA: semiconductor optical amplifier
SSMF: standard single-mode fiber
VOA: variable optical attenuator

Figure 7. 20 km 25 GBaud PAM4 single sideband modulation-direct detection point-to-point downlink experimental platform

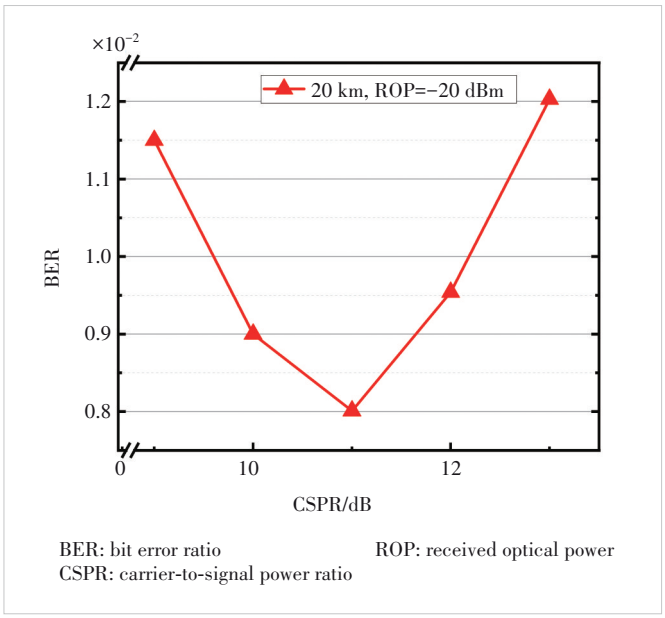

BER: bit error ratio
CSPR: carrier-to-signal power ratio
ROP: received optical power

Figure 8. BER vs CSPR for 20 km transmission experiment

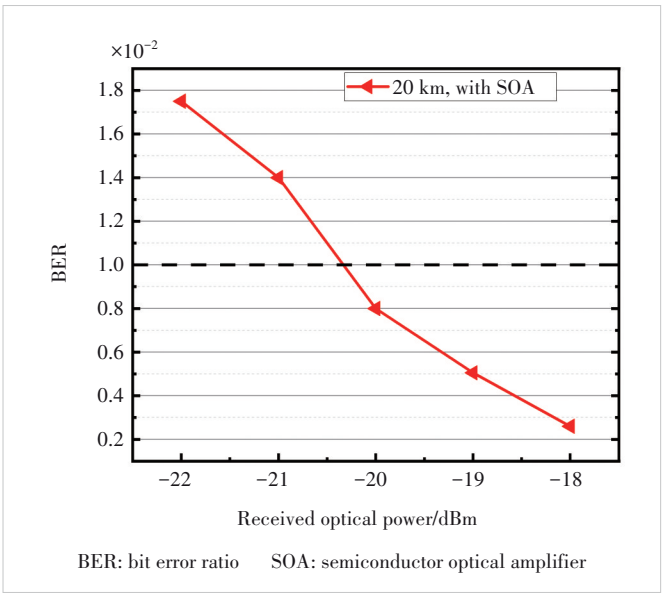

BER: bit error ratio
SOA: semiconductor optical amplifier

Figure 9. BER vs ROP under a 20 km transmission experiment

was adopted in subsequent experiments.

Fig. 9 shows how BER varies with ROP. Under the current experimental conditions, the receiver sensitivity of the 20 km transmission experimental system is −20.4 dBm. At this sensitivity, the second-order Volterra equalizer employs 91 linear taps and 21 second-order taps, and the overall power budget of the system is 30.4 dB. At 1550 nm (where dispersion is greater than 300 ps/nm), the quadratic Volterra equalizer is considered effective. Ref. [15] demonstrates a PON system with real-time transmission of 50 Gbit•s^{-1}•λ^{-1} PAM4 using a booster SOA. This system achieves a sensitivity of −22.3 dBm at a BER of 10^{-2}, with a power budget higher than 35 dB across the O-band. The performance of this experiment is essentially comparable to, though slightly lower than, the results reported in Ref. [15]. The gap is attributed to the single sideband modulation method, operating wavelength, bandwidth limitations, and SOA amplifier performance.

5 Conclusions

In this paper, a 200 Gbit/s Nyquist PAM4 SSB-DD downlink system scheme is proposed and demonstrated, and a low-complexity QNLE is proposed for low complexity nonlinear im-

pairment equalization, which can greatly reduce the computational complexity of the conventional VNLE by keeping only the primary linear terms and quadratic nonlinear terms. Simulation results for the 200 Gbit/s SSB-DD downlink system show that the computational complexity of the quadratic nonlinear equalizer is about 28% of that of the conventional Volterra nonlinear equalizer. The proposed QNLE exhibits excellent nonlinear equalization ability, as it achieves a power budget of 29 dB under the 20 km fiber transmission, while a power budget of 30.4 dB is achieved in the 50 Gbit/s experiment. It is concluded that the proposed SSB-DD PON scheme with reduced complexity quadratic Volterra equalization algorithm yields superior system performance, and thus is one of the most promising solutions for future 200 Gbit/s PON applications.

References

[1] Houtsma V, Van Veen D. High speed optical access networks for this decade and the next (invited) [C]//IEEE Photonics Conference (IPC). IEEE, 2022: 1 – 2. DOI: 10.1109/IPC53466.2022.9975573
[2] Gao Y L, Cartledge J C, Kashi A S, et al. Direct modulation of a laser using 112-Gb/s 16-QAM nyquist subcarrier modulation [J]. IEEE photonics technology letters, 2017, 29(1): 35 – 38. DOI: 10.1109/lpt.2016.2627000
[3] Xue L, Lin R, Van Kerrebrouck J, et al. 100G PAM-4 PON with 34 dB power budget using joint nonlinear tomlinson-harashima precoding and Volterra equalization [C]//European Conference on Optical Communication (ECOC). IEEE, 2021: 1 – 4. DOI: 10.1109/ecoc52684.2021.9606041
[4] Wang W Y, Li H L, Zhao P C, et al. Advanced digital signal processing for reach extension and performance enhancement of 112 Gbit/s and beyond direct detected DML-based transmission [J]. Journal of lightwave technology, 2019, 37(1): 163 – 169. DOI: 10.1109/JLT.2018.2885707
[5] Xie C J, Dong P, Randel S, et al. Single-VCSEL 100-Gb/s short-reach system using discrete multi-tone modulation and direct detection [C]//Optical Fiber Communication Conference. OSA, 2015: Tu2H. 2. DOI: 10.1364/ofc.2015.tu2h.2
[6] Sun L, Du J B, He Z Y. Multiband three-dimensional carrierless amplitude phase modulation for short reach optical communications [J]. Journal of lightwave technology, 2016, 34(13): 3103 – 3109. DOI: 10.1109/JLT.2016.2559783
[7] Xiang M, Fu S N, Xu O, et al. Advanced DSP enabled C-band 112 Gbit/s/λ PAM-4 transmissions with severe bandwidth-constraint [J]. Journal of lightwave technology, 2022, 40(4): 987 – 996. DOI: 10.1109/jlt.2021.3125336
[8] Zhong F, Gong P, Zhou Z P, et al. High performance optical modulator and detector for 100 Gbit/s transmission system [J]. ZTE communications, 2017, 15(3): 46 – 51. DOI: 10.3969/j.issn.16735188.2017.03.006
[9] Yan B L, Wu Q, Shi H, et al. Toward low-cost flexible intelligent OAM in optical fiber communication networks [J]. ZTE communications, 2022, 20 (3): 54 – 60. DOI: 10.12142/ZTECOM.202203007
[10] Tang X Z, Qiao Y J, Chang G K. Experimental demonstration of C-band 112-Gb/s PAM4 over 20-km SSMF with joint pre- and post-equalization [C]//Optical Fiber Communication Conference (OFC) 2020. Optica Publishing Group, 2020. DOI: 10.1364/ofc.2020.w2a.46
[11] Tang X Z, Zhou J, Guo M Q, et al. An efficient nonlinear equalizer for 40-Gb/s PAM4-PON systems [C]//Proceedings of Optical Fiber Communication Conference. OSA, 2018: 1 – 3. DOI: 10.1364/ofc.2018.w2a.62
[12] Chagnon M. Optical communications for short reach [C]//European Conference on Optical Communication (ECOC). IEEE, 2018: 1 – 3. DOI: 10.1109/ECOC.2018.8535355
[13] Kaneda N, Lee J, Chen Y K. Nonlinear equalizer for 112-Gb/s SSB-PAM4 in 80-km dispersion uncompensated link [C]//Proceedings of Optical Fiber Communication Conference. OSA, 2017: 1 – 3. DOI: 10.1364/ofc.2017.tu2d.5
[14] Yu Y K, Choi M, Bo T W, et al. Low-complexity quadratic equalizer for DML-based IM/DD systems [C]//Proceedings of 24th OptoElectronics and Communications Conference (OECC) and 2019 International Conference on Photonics in Switching and Computing (PSC). IEEE, 2019: 1 – 3. DOI: 10.23919/PS.2019.8817645
[15] Lee H H, Kim K, Doo K H, et al. Demonstration of high-power budget TDM-PON system with 50 Gb/s PAM4 and saturated SOA [J]. Journal of lightwave technology, 2021, 39(9): 2762 – 2768. DOI: 10.1109/JLT.2021.3059902

Biographies

Yang Tao (yangtao@bupt.edu.cn) is an associate professor at the School of Electronic Engineering, Beijing University of Posts and Telecommunications (BUPT), China. He received his PhD degree in information and communication engineering from BUPT in 2019, followed by a postdoctoral fellowship in Electronic Science and Technology. His research interests include ultra-high-speed optical transmission, digital signal processing algorithms for optical communications, and intelligent optical network monitoring and management. He has authored or co-authored over 70 papers in prestigious journals and conferences like Optics Express and OFC, and holds more than 12 patents. He also serves as a guest editor and reviewer for several international journals.

Huang Xingang is a senior expert in technical pre-research with the Fixed Network Product Line, ZTE Corporation. He has long been engaged in the research and standardization of optical access technologies.

Ma Zhuang is the Head of Fixed Network Product Technology Pre-Research Department at ZTE Corporation. His work focuses on the pre-research, planning, and development of fixed broadband and optical access products. He has published more than 10 technical papers and is the inventor of over 20 granted patents.

Zhong Yiming is a senior engineer with the Fixed Network Pre-research Department, ZTE Corporation. His research centers on the R&D and innovation of PON products, with a primary focus on 50G PON system architecture design and algorithm research. He actively participates in PON standardization in ITU-T SG15, CCSA, and other industrial standards organizations, and has submitted numerous international standard contributions. He holds rich technical expertise in PON systems and has been granted multiple national invention patents.

Huang Xiatao is currently a technology research engineer at ZTE Corporation. He received his PhD degree in information and communication engineering from University of Electronic Science and Technology of China in 2023. His research interests include ultra-high-speed optical transmission, digital signal processing algorithms for optical coherent communications, and optical intelligent access system. He has held more than 6 patents.

Liu Bo is a chief pre-research engineer of OAN Product Line, ZTE Corporation. His research focuses on the pre-research of PON technologies.